Structure of PSI, PSII and antennae complexes from yellow-green alga Xanthonema debile

ARTICLE *in* PHOTOSYNTHESIS RESEARCH · MARCH 2011

Impact Factor: 3.5 · DOI: 10.1007/s11120-011-9647-z · Source: PubMed

3 AUTHORS, INCLUDING:

Josef Tichý
University of South Bohemia in České Bud…
6 PUBLICATIONS **38** CITATIONS
SEE PROFILE

Frantisek Vacha
University of South Bohemia in České Bud…
74 PUBLICATIONS **765** CITATIONS
SEE PROFILE

Photosynth Res (2011) 108:25–32
DOI 10.1007/s11120-011-9647-z

REGULAR PAPER

Structure of PSI, PSII and antennae complexes from yellow-green alga *Xanthonema debile*

Zdenko Gardian · Josef Tichý · František Vácha

Received: 26 October 2010 / Accepted: 16 March 2011 / Published online: 31 March 2011

Abstract Photosynthetic carbon fixation by Chromophytes is one of the significant components of a carbon cycle on the Earth. Their photosynthetic apparatus is different in pigment composition from that of green plants and algae. In this work we report structural maps of photosystem I, photosystem II and light harvesting antenna complexes isolated from a soil chromophytic alga *Xanthonema debile* (class Xanthophyceae). Electron microscopy of negatively stained preparations followed by single particle analysis revealed that the overall structure of Xanthophytes' PSI and PSII complexes is similar to that known from higher plants or algae. Averaged top-view projections of Xanthophytes' light harvesting antenna complexes (XLH) showed two groups of particles. Smaller ones that correspond to a trimeric form of XLH, bigger particles resemble higher oligomeric form of XLH.

Keywords Photosynthesis · Chromophytes · *Xanthonema debile* · Photosystem I · Photosystem II · FCP · Electron microscopy

Abbreviations

Chl	Chlorophyll
HEPES	4-(2-Hydroxyethyl)-1-piperazineethanesulfonic acid
DEAE	Diethyaminoethyl
DM	*n*-Dodecyl-*β*-D-maltoside
EM	Electron microscopy
FCP	Fucoxanthin-chlorophyll proteins
LHCI	Light-harvesting complex of photosystem I
LHCII	Light-harvesting complex of photosystem II
PSI	Photosystem I
PSII	Photosystem II
SDS-PAGE	Polyacrylamide gel electrophoresis in the presence of sodium dodecylsulfate

Introduction

The Chromophytes (Heterokont) contribute significantly to the photosynthetic carbon fixation in oceans. Except water, some classes inhabit also soil environments. *Xanthonema debile* is an example of unique soil chromophytic alga that differs from not only green plants and algae but also other Chromophytes. Such differences have been extensively studied previously. There are no grana stackings and no segregation of photosystems (Pyszniak and Gibbs 1992) within its thylakoid membranes. Photosynthetic apparatus contains Chl a, *β*-carotene, diadinoxanthin, diatoxanthin, heteroxanthin, and vaucheriaxanthinester. Xanthophyceae may also contain chlorophyll c, but usually only in very small amount (Baldisserotto et al. 2005). Fucoxanthin, the main light-harvesting carotenoid present in other Chromophytes classes, is absent in Xanthophyceae (Bailey and

Electronic supplementary material The online version of this article (doi:10.1007/s11120-011-9647-z) contains supplementary material, which is available to authorized users.

Z. Gardian · F. Vácha
Biology Centre ASCR, Branišovská 31, 370 05 České Budějovice, Czech Republic

Z. Gardian · F. Vácha (✉)
Institute of Physical Biology, University of South Bohemia, Zámek 136, 373 33 Nové Hrady, Czech Republic
e-mail: vacha@jcu.cz

J. Tichý · F. Vácha
Faculty of Science, University of South Bohemia, Branišovská 31, 370 05 České Budějovice, Czech Republic

Andersen 1998; Van den Hoek et al. 1995; Buchel and Garab 1997).

Since fucoxanthin is the most prominent carotenoid in the majority of Chromophytes, their light harvesting antenna proteins are usually called fucoxanthin-chlorophyll proteins (FCP). The chromophytic FCP are usually smaller (17–24 kDa) than the light-harvesting complexes (LHC) of plants and green algae (Hiller et al. 1991; Caron et al. 1987; Buchel 2003). Several years ago, one type of FCP for both photosystems has been purified from Chromophytes (Berkaloff et al. 1990; Owens and Wold 1986; Katoh et al. 1989; Passaquet et al. 1991; De Martino et al. 1997), recently trimeric and higher oligomeric state of Chromophytes FCP complexes were described in Diatoms (Buchel 2003; Beer et al. 2006; Guglielmi et al. 2005; Brakemann et al. 2006). Xanthophytes do not contain fucoxanthin, therefore, we are using, in this work, the term Xanthophytes' light-harvesting (XLH) complexes instead of FCP.

Electron microscopy (EM) followed by a single particle analysis offers a powerful tool to visualise and study structure of large proteins and protein complexes. This method brought already number of structural data of photosynthetic pigment–protein complexes during last decades. For example at the end of 80s single particle analysis showed that cyanobacterial PSI occurs preferably in trimeric form (Boekema et al. 1987; Ford and Holyenburg 1988; Rogner et al. 1990), trimers of PSI were observed in Prochlorophyta (van der Staay et al. 1993; Bibby et al. 2001; Bumba et al. 2005) that are very close to cyanobacteria. Compared to the PSI trimers green alga, red alga and higher plants showed PSI only as a monomeric particle with half-moon shaped LHCI antenna on one side of the PSI complex (Boekema et al. 2001; Germano et al. 2002; Kargul et al. 2003; Gardian et al. 2007). The EM structural studies of cyanobacterial and spinach PSII (Boekema et al. 1995) showed a dimeric organisation of PSII core complexes. Small protrusions on the lumenal side of the PSII complexes were attributed to the extrinsic proteins of the oxygen-evolving complex (Kuhl et al. 1999; Bumba et al. 2004a). Electron microscope was also used to study structural organisation of higher plants PSII and their light-harvesting antennae (LHCII). LHCII was found as a two trimeric and four monomeric complexes around the dimeric PSII core complex (Boekema et al. 1995). Except this, higher order supercomplexes of PSII–LHCII were also found in higher plants forming megacomplexes, in which PSII is associated with different numbers of LHCII in different positions (Boekema et al. 1999).

In contrast, the number of information about the organisation of higher plants, algae or cyanobacteria photosynthetic complexes and their LHC, there are no such structural data obtained for Chromophytes' photosynthetic apparatus. Only one record has been published on FCP-antennae of Diatoms showing PSI–FCP complex in the EM micrograph as a monomer (Veith and Buchel 2007), however, no particle analysis has been done in this study.

In this contribution we report structural maps of PSI and PSII complexes and light harvesting antennae isolated from the unique chromophytic alga *Xanthonema debile*. We have also characterised the organisation of PSI and PSII complexes with a particular respect to the arrangement of light harvesting antennae complexes.

Materials and methods

The chromophytic alga *Xanthonema debile* was batch cultivated in 5 l flasks at room temperature in Bold-Basal/Bristol (BBM) medium (Bischoff and Bold 1963) and bubbled with filtered air. The light irradiance was 100 μmol photon m^{-2} s^{-1}. Cells were harvested by centrifugation at 1,800×*g* for 5 min, washed with distilled water, and resuspended in a buffer containing 10 mM HEPES (pH 7.4), 2 mM $MgCl_2$, 2 mM $MnCl_2$, 10 mM KCl, 1 M sorbitol and inhibitors of chlorophyllase and proteases (10 mM hydroxymercuri benzoic acid sodium salt, 1 mM benzamidine and 1 mM phenylmethanesulfonylfluoride).

Cells were broken by a double French press cycle at 15,000 psi. The unbroken cells were removed by centrifugation for 5 min at 3,000×*g*. The supernatant was then centrifuged for 1 h at 60,000×*g* to pellet thylakoid membranes. Membranes were resuspended and solubilised with 5% Digitonin at a chlorophyll concentration of 1 mg (Chl) ml^{-1} for 60 min. The unsolubilised material was removed by centrifugation for 20 min at 60,000×*g* and the supernatant was loaded onto DEAE Sepharose CL-6B (Amersham Biosciences, Sweden) anion-exchange column equilibrated with 10 mM HEPES (pH 7.4), 2 mM $MgCl_2$, 2 mM $MnCl_2$, 0.03% DM. Photosynthetic complexes were eluted from the column by a salt gradient at a concentration of about 120 mM NaCl and loaded onto a fresh 0–1.2 M continuous sucrose density gradient prepared by freezing and thawing the centrifuge tubes filled with a buffer containing 10 mM HEPES (pH 7.4), 2 mM $MgCl_2$, 2 mM $MnCl_2$, 10 mM KCl, 0.03% DM, 0.6 M sucrose. The following centrifugation was carried out at 4°C using a P56ST swinging rotor (Sorvall) at 150,000×*g* for 14 h. After centrifugation the sample was separated into a zone with light-harvesting antennae and a zone with a mixture of PSI and PSII core complexes. Zones resolved in the sucrose density gradient were further desalted by a gel filtration using Sephadex G-25 (Amersham Biosciences, Sweden), which also reduced the amount of sucrose and improved a contrast in EM.

Chlorophyll concentration was determined according to Ogawa and Vernon (1971). Room temperature absorption

spectra were recorded with a UV300 spectrophotometer (Spectronic Unicam, Cambridge, UK). Fluorescent emission spectra were measured at a liquid nitrogen temperature using a Fluorolog-2 spectrofluorometer (Jobin–Yvon, Edison, NJ, USA) with an excitation wavelength of 435 nm and a chlorophyll concentration of 10 μg (Chl) ml^{-1}. The protein composition was determined by SDS-PAGE using a 12.5% polyacrylamide gel containing 6 M urea and stained with Coomassie Brilliant Blue or with silver staining.

Pigment composition was analysed by high-performance liquid chromatography (HPLC) consisting of Pump Controller 600, Delta 600 injection system and a PDA 996 detector (Waters, USA). Pigments were separated on a reverse phase ZORBAX ODS column (4.5 × 250 mm, 5 μm, non-endcapped) using a binary solvent system (0 min 40% A, 60% B, 15 min 100% B, 35 min 100% B; where the solvent A is 70% 0.5 M ammonium acetate in methanol, B is 40% acetone in methanol). Flow rate was 1.5 ml min^{-1}. The photosynthetic pigment molar ratios were estimated from areas under corresponding chromatogram peaks displayed at wavelengths corresponding to the particular extinction coefficient. The molar extinction coeficients ε (dm^3 $mmol^{-1}$ cm^{-1}) were 79.4 for Chl a at 665 nm, 131 for Diadinoxanthin at 444 nm, 119 for Diatoxanthin at 452 nm, 131 for Heteroxanthin at 444 nm and 141 for vaucheriaxanthinester at 453 nm (Lichtenthaler 1987; Koblizek, personal communication).

Freshly prepared photosynthetic complexes were immediately used for EM. The specimen was placed on glow-discharged carbon-coated copper grids and negatively stained with 2% uranyl acetate. EM was performed with JEOL 1010 transmission electron microscope (JEOL, Japan) using 80 kV at 60,000× magnification. EM micrographs were digitized with a pixel size corresponding to 5.1 Å at the specimen level. Image analyses were carried out using Spider and Web software package (Frank et al. 1996). The selected projections were rotationally and translationally aligned, and treated by multivariate statistical analysis in combination with classification procedure (van Heel and Frank 1981; Harauz et al. 1988). Classes from each of the subsets were used for refinement of alignments and subsequent classifications. For the final sum, the best of the class members were summed using a cross-correlation coefficient of the alignment procedure as a quality parameter.

Results and discussion

PSII and PSI complexes from chromophytic algae have been previously isolated using sucrose density gradient centrifugation (Ikeda et al. 2008; Brakemann et al. 2006) or ion exchange chromatography (Veith and Buchel 2007; Douady et al. 1993). In order to isolate pure photosynthetic complexes from *Xanthonema debile*, we have combined both techniques. At first, ion exchange chromatography was used to obtain purified mixture of PSI, PSII and XLH antennae complexes from digitonin solubilised thylakoid membranes. In the second step, sucrose density gradient centrifugation separated the sample into two zones of free XLH and a mixture of PSI, PSII complexes.

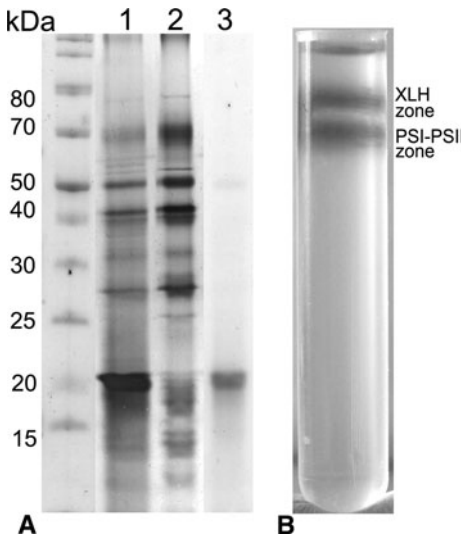

Fig. 1 **a** SDS-PAGE analysis of pigment–protein complexes from thylakoid membranes of *Xanthonema debile*. *Lane* (*1*) represents PSI–PSII–XLH fraction eluted from DEAE Sepharose CL-6B anion-exchange column with 120 mM NaCl. (*2*) Purified PSI–PSII zone and (*3*) XLH zone resolved after sucrose density gradient centrifugation of PSI–PSII–XLH obtained by anion-exchange cromatography. **b** Sucrose density gradient of PSI–PSII–XLH fraction. The sample was divided into two zones containing free XLH antennae and a mixture of PSI and PSII core complexes

From DEAE Sepharose CL-6B anion-exchange column, two chlorophyll-containing fractions were eluted with a linear gradient of 0–600 mM NaCl. The first fraction can be attributed to free pigments. The second fraction eluted with 120 mM NaCl contained polypeptides of PSI, PSII complexes and light-harvesting antennae (XLH) as indicated by SDS-PAGE (Fig. 1a, line 1). This fraction contained a 60 kDa band typical for the PsaA/B reaction centre proteins of PSI, and protein bands characteristic for the PSII, the intrinsic antennae CP47, CP43 and reaction centre proteins D2 and D1. Such protein composition is uniform in all eukaryotic algae (Wilhelm et al. 1988). SDS gels show also a prominent band about 20 kDa, corresponding to antenna polypeptides of XLHs (Hiller et al. 1991; Caron et al. 1987; Buchel 2003; Joshi-Deo et al. 2010).

The second fraction from anion-exchange column chromatography was loaded onto a sucrose density gradient. After 14 h centrifugation at 150,000×*g* the sample was separated into two zones (Fig. 1b). SDS-PAGE analysis

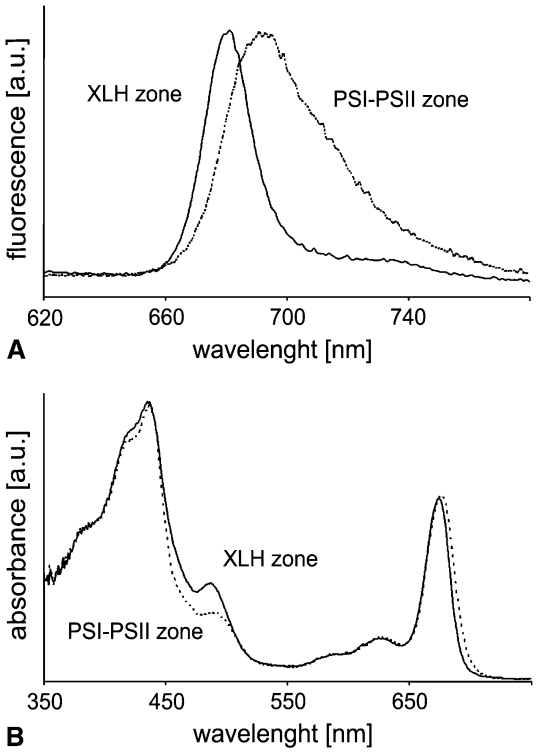

Fig. 2 77 K fluorescence emission spectra (**a**) and absorption spectra (**b**) of sucrose density gradient zones. The XLH (*solid line*) and PSI–PSII (*dashed line*) zones were obtained by a sucrose density gradient centrifugation of PSI–PSII–XLH anion-exchange fraction. Spectra are normalised to their maxima

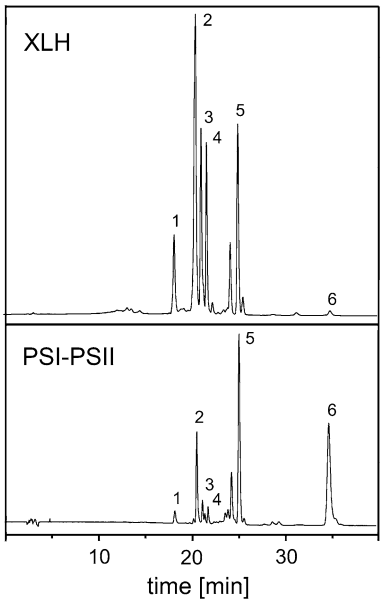

Fig. 3 HPLC chromatograms of XLH and PSI–PSII zones. Chromatograms consist of vaucheriaxanthinester eluted at ~15 min (peak number *1*), diadinoxanthin at ~18 min (*2*), diatoxanthin at ~19 min (*3*), heteroxanthin at ~20 min (*4*), chlorophyll a at ~25 min (*5*) and *β*-carotene (*6*) at ~35 nim. Chromatograms were detected at 450 nm and normalised to the amplitude of the chlorophyll a peak at 25 min

showed that the bottom zone contained mainly PSI and PSII core complexes while the upper zone contained free XLH antennae (Fig. 1a, lanes 2 and 3). This result corresponds to previous reports of separation of chromophytes pigment protein complexes on sucrose density gradient into PSI–PSII and FCP zone (Lepetit et al. 2007; Joshi-Deo et al. 2010).

77 K fluorescence emission spectra of sucrose density gradient zones are shown in Fig. 2a. The upper XLH zone is characterised by a peak at 682 nm, a typical region of fluorescence emission of FCP antennae. The bottom zone peaks at 691 nm, corresponding to the emission of PSII, with a broad long wavelength shoulder of the emission of PSI. The significant long-wavelength fluorescence component found in many species is missing probably due to the absence of specific "red" chlorophyll molecules (Gobets and van Grondelle 2001) as it was reported previously in, e.g. some cyanobacteria (Mimuro et al. 2002; Koenig and Schmidt 1995), and red algae (Grabowski et al. 2000).

Room temperature absorption spectra of the PSI–PSII zone and XLH zone are in Fig. 2b, showing higher content of carotenoids in the XLH antennae zone.

Figure 3 shows HPLC chromatograms of the PSI–PSII zone and XLH zone detected at 450 nm. Chromatograms consisted of four xanthophile peaks with retention time between 14 and 22 min (vaucheriaxanthinester (1), diadinoxanthin (2), diatoxanthin (3), heteroxanthin (4)), chlorophyll a (5) peak with retention time around 25 min and *β*-carotene (6) at 35 min. Chlorophyll c, another accessory light-harvesting pigment can be present in Chromophytes in very different amount (Whittle and Casselton 1975; Green and Parsons 2003), and in some species it is hard to detect, especially when it is not specifically looked for. *X. debile* is such an example of chromophytic alga with negligible amount of chlorophyll c.

Photosynthetic pigment molar ratio of purified PSI–PSII zone was calculated to be 131 (Chl a):11 (Diadino):2 (Diato):2 (Hetero):1 (Vauch):28 (*β*-car). In comparison, the molar ratio of the pigment molecules in the XLH zone was calculated to be 28 (Chl a):11 (Diadino):5 (Diato):4 (Hetero):1 (Vauch):0 (*β*-car). The ammount of *β*-carotene in the PSI–PSII zone was slightly dependent on growing conditions and collection period. Traces of *β*-carotene were detectable also in the XLH zone, however, the ammount was very low and most probably due to a slight contamination from the background of the second sucrose density gradient zone containing photosystem I and II.

Purified photosynthetic complexes were negatively stained by 2% uranyl acetate, visualised by EM and processed by image analysis. Typical EM images of PSI–PSII

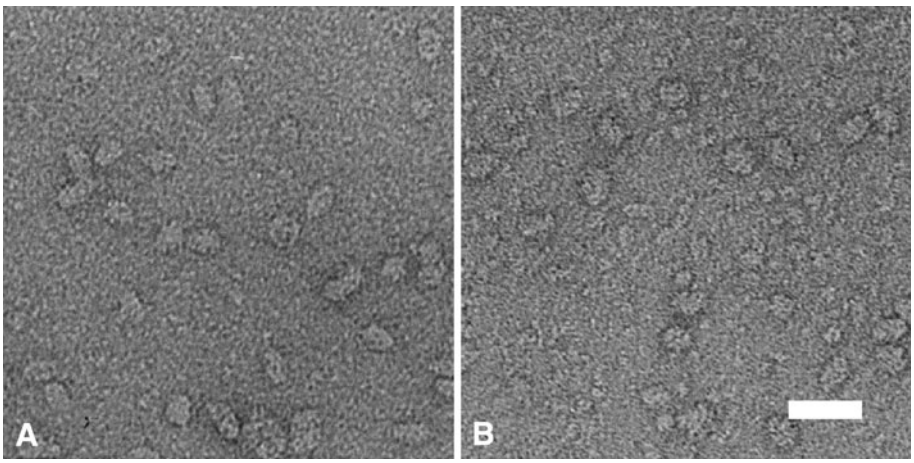

Fig. 4 Electron micrographs of **a** PSI–PSII and **b** XLH complexes in their top-view projections. Samples were negatively stained with 2% uranyl acetate. The *scale bar* represents 50 nm

and XLH zone are shown in Fig. 4. To process the particle images by single particle analysis, we have selected 6900 particles from the images of PSI–PSII zone and 6120 particles from XLH zone. The selected projections were aligned, treated with multivariate statistical analysis and classified into classes. After the classification steps, selected photosynthetic complexes were decomposed into 15 and 18 classes for PSI–PSII and XLH zones, respectively.

The projections of PSI–PSII zone can be divided into two groups of particles shown in Fig. 5a, b and c, d, respectively. The first group (Fig. 5a, b) had an oval shape and represents monomeric PSI core complexes. PSI from *X. debile* did not reveal dimeric or trimeric form of PSI particles as found in cyanobacteria (Kruip et al. 1997). The size and shape of these particles are very similar to the PSI core complexes previously observed in algae (Germano et al. 2002; Kargul et al. 2003; Bumba et al. 2004a; Gardian et al. 2007) or higher plants (Boekema et al. 2001). Figure 6a presents the most representative class average of 524 top-view projections of PSI complexes, overlaid with an X-ray structure of PsaA/B heterodimer of PSI from *Synechococcus elongatus* (Jordan et al. 2001).

The top-view projections of the second group of particles from PSI–PSII zone show diamond-shaped particles with twofold rotational symmetry (Fig. 5c, d). These particles resemble the PSII core complexes isolated from cyanobacteria, algae and higher plants (Boekema et al. 1995; Kuhl et al. 1999; Bumba et al. 2004a; b; Vacha et al. 2005). Class average of 281 top-view projections of PSII complexes is shown in Fig. 6b. The PSII particle is overlaid with PSII crystal structure obtained from *Thermosynechococcus elongatus* (Loll et al. 2005). A comparison of amount of the PSII and PSI complexes in electron micrographs shows that only a few PSII complexes are fixed to the EM grids compared to the PSI. However, it is hard to speculate on the number of PSI and PSII complexes in the

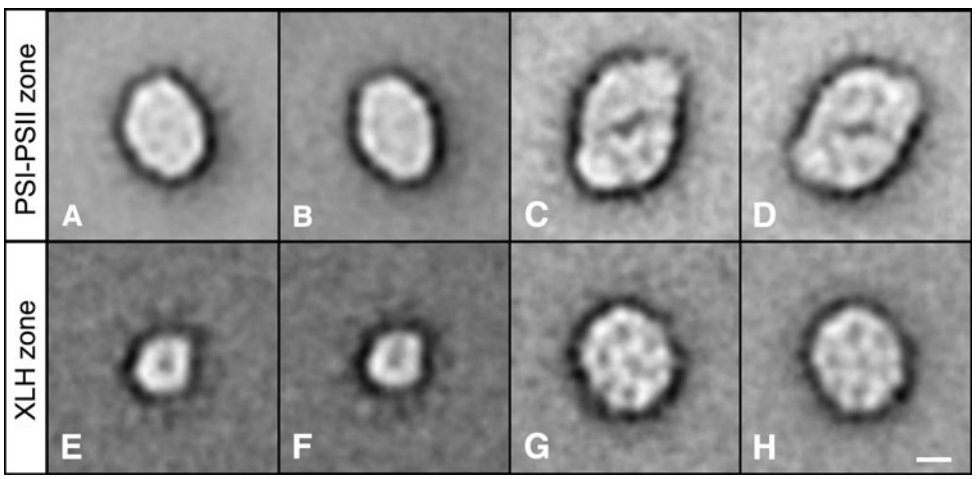

Fig. 5 Single particle analysis of top-view projection maps of *X. debile* photosynthetic pigment–protein complexes. **a–d** The most representative class averages obtained by classification of 6900 particles from the PSI–PSII sucrose density gradient zone. **e–h** The most representative class averages obtained by classification of 6120 particles from the XLH sucrose density gradient zone. The number of summed images is: 524 (**a**), 486 (**b**), 258 (**c**), 281 (**d**), 442 (**e**), 412 (**f**), 322 (**g**) and 356 (**h**). The *scale bar* represents 5 nm

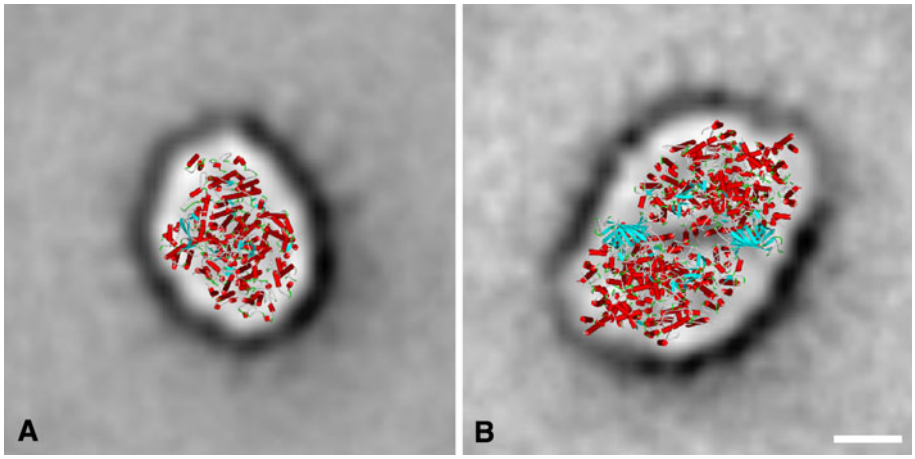

Fig. 6 Schematic representation of the overal structure of the PSI and PSII complexes isolated from *X. debile*. The most representative top-view PSI (**a**) and PSII (**b**) projection maps of negatively stained particles from PSI–PSII sucrose density gradient zone. The projections are overlaid with a cyanobacterial X-ray model of the PSI (**a**) and PSII (**b**) core complexes. The coordinates are taken from Protein Data Bank (http://www.rcsb.org/pdb). **a** Code 1JB0 and **b** code 2AXT. The *scale bar* represents 5 nm

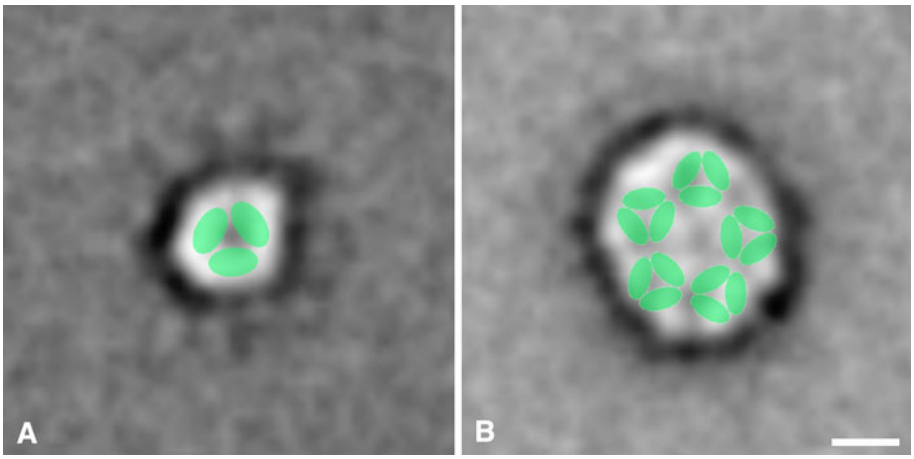

Fig. 7 Schematic representation of the XLH subunits organisation in XLH complexes isolated from *X. debile*. **a** The most representative class averages of top-view trimeric XLH projections overlaid with a model of XLH trimer. **b** The most representative class averages of top-view projections of oligomeric XLH overlaid with a model of five trimeric XLH. The *scale bar* represents 5 nm

thylakoid membrane because PSII lumenal surface has a much lower affinity to the support carbon film than PSI (Boekema et al. 1995; Kuhl et al. 1999).

The most representative classes of single particle analysis of XLH complexes are in Fig. 5e, h. Other studies showed that FCP complexes can be organised in a trimeric or even higher oligomeric states (Buchel 2003; Beer et al. 2006; Guglielmi et al. 2005; Brakemann et al. 2006). Our averaged top-view projections of XLH show two groups of particles. The smaller one, with a size of about 7 nm, corresponds to the trimeric form of XLH. Figure 7a represents class average of this trimeric XLH, made of 442 summed images and overlaid with a model of trimeric FCP (Buchel 2003). The bigger particles (about 12 nm) had an oval shape and resemble the higher oligomeric form of XLH. It was reported that such higher oligomers can consist of six to nine monomers of FCP (Buchel 2003), but oligomers of even seven trimers were suggested on the bases of calculations (Mimuro et al. 1990; Katoh and Ehara 1990). Our results suggest five trimers in one oligomeric XLH. The incorporation of the five trimeric XLH antennae into the most representative class average of 356 top-view projections of oligomeric XLH complexes is shown in Fig. 7b.

In this paper we have confirmed that the overall structure of PSI and PSII reaction centres from unique alga *X. debile*, which belongs to Chromophytic class Xanthophyceae, is similar to that known from higher plants or algae. We have also demonstrated the structure of trimeric and higher oligomeric forms of XLHs, obtained by EM and single particle image analysis. Since we were, despite increased effort, not able to obtain photosynthetic reaction centres associated with light-harvesting antenna XLH, the question how XLH antennae are bound to PSI or PSII, or whether they are attributed to a certain photosystem at all remains open.

Acknowledgments Authors would like to thank F. Matoušek and I. Hunalová for their technical support. We gratefully acknowledge the financial support of the Ministry of Education, Youth and Sports of the Czech Republic MSM6007665808, AV0Z50510513, and Grant GAAV IAA601410907.

References

Bailey JC, Andersen RC (1998) Phylogenetic relationships among nine species of the Xanthophyceae inferred from rbc L and 18S rRNA gene sequences. Phycologia 37:458–466

Baldisserotto C, Ferroni L, Moro I, Fasulo MP, Pancaldi S (2005) Modulations of the thylakoid system in snow xanthophycean alga cultured in the dark for two months: comparison between microspectrofluorimetric responses and morphological aspects. Protoplasma 226:125–135

Beer A, Gundermann K, Beckmann J, Buchel C (2006) Subunit composition and pigmentation of fucoxanthin-chlorophyll proteins in diatoms: evidence for a subunit involved in diadinoxanthin and diatoxanthin binding. Biochemistry 45:13046–13053

Berkaloff C, Caron L, Rousseau B (1990) Subunit organization of PS I particles from brown algae and diatoms: polypeptide and pigment analysis. Photosynth Res 23:181–193

Bibby TS, Nield J, Partensky F, Barber J (2001) Oxyphotobacteria-antenna ring around photosystem I. Nature 413:590

Bischoff HW, Bold HC (1963) Phycological studies IV. Some soil algae from enchanted rock and related algal species. Univ Texas Publ 6318:1–95

Boekema EJ, Dekker JP, van Heel MG, Rogner M, Saenger W, Witt I, Witt HT (1987) Evidence for a trimeric organization of the photosystem I complex from the thermophilic cyanobacterium *Synechococcus* sp. FEBS Lett 217:283–286

Boekema EJ, Hankamer B, Bald D, Kruip J, Nield J, Boonstra AF, Barber J, Rogner M (1995) Supramolecular structure of the photosystem II complex from green plants and cyanobacteria. Proc Natl Acad Sci USA 92:175–179

Boekema EJ, van Roon H, Calkoen F, Bassi R, Dekker JP (1999) Evidence multiple types of association of photosystem II and its light-harvesting antenna in partially solubilized photosystem II membranes. Biochemistry 38:2233–2239

Boekema EJ, Hifney A, Yakushevska AE, Piotrowski M, Keegstra W, Berry S, Michael KP, Pistorius EK, Kruip J (2001) A giant chlorophyll-protein complex inducted by iron deficiency in cyanobacteria. Nature 412:745–748

Brakemann T, Schlormann W, Marquardt J, Nolte M, Rhiel E (2006) Association of fucoxanthin chlorophyll a/c-binding polypeptides with photosystems and phosphorylation in the centric diatom *Cyclotella cryptica*. Protist 157:463–475

Buchel C (2003) Fucoxanthin-chlorophyll proteins in diatoms: the 18 kDa and 19 kDa subunits assemble into different oligomeric states. Biochemistry 42:13027–13034

Buchel C, Garab G (1997) Organization of the pigment molecules in the chlorophyll a/c light-harvesting complex of *Pleurochloris meiringensis* (Xanthophyceae) characterization with circular dichroism and absorbance spectroscopy. J Photochem Photobiol B: Biol 37:118–124

Bumba L, Husak M, Vacha F (2004a) Interaction of PSII–LHCII supercomplexes in adjacent layers of stacked chloroplast thylakoid membranes. Photosynthetica 42:193–199

Bumba L, Havelkova-Dousova H, Husak M, Vacha F (2004b) Structural characterization of photosystem II complex from red alga *Porphyridium cruentum* retaining extrinsic subunits of the oxygen-evolving complex. Eur J Biochem 271:2967–2975

Bumba L, Prasil O, Vacha F (2005) Antenna ring around trimeric photosystem I in chlorophyll b containing cyanobacterium *Prochlorothrix hollandica*. Biochim Biophys Acta 1708:1–5

Caron L, Remy R, Berkaloff C (1987) Polypeptide composition of light-harvesting complexes from some brown algae and diatoms. FEBS Lett 229:11–15

De Martino A, Douady D, Rousseau B, Duval JC, Caron L (1997) Characterization of two light-harvesting subunits isolated from the brown alga *Pelvetia canaliculata*: heterogeneity of xanthophyll distribution. Photochem Photobiol 66:190–197

Douady D, Rousseau B, Berkaloff C (1993) Isolation and characterization of PSI core complexes from a brown alga, *Laminaria saccharina*. FEBS Lett 324:22–26

Ford RC, Holyenburg A (1988) Investigation of the structure of trimeric and monomeric photosystem I reaction center complex. EMBO J 7:2287–2293

Frank J, Radermacher M, Penczek P, Zhu J, Li YH, Ladjadj M, Leith A (1996) SPIDER and WEB: processing and visualization of images in 3D electron microscopy and related fields. J Struct Biol 116:190–199

Gardian Z, Bumba L, Schrofel A, Herbstova M, Nebesarova J, Vacha F (2007) Organisation of photosystem I and photosystem II in red alga *Cyanidium caldarium*: encounter of cyanobacterial and higher plant concepts. Biochim Biophys Acta 1767:725–731

Germano M, Yakushevska AE, Keegstra W, van Gorkom HJ, Dekker JP, Boekema EJ (2002) Supramolecular organization of photosystem I and light-harvesting complex I in *Chlamydomonas reinhardtii*. FEBS Lett 525:121–125

Gobets B, van Grondelle R (2001) Energy transfer and trapping in photosystem I. Biochim Biophys Acta 1507:80–99

Grabowski B, Tan S, Cunningham FX, Gantt E (2000) Characterization of the *P. cruentum* Chl a-binding LHC by in vitro reconstitution: LHCaR1 binds 8 Chl a molecules and proportionately more carotenoids than CAB proteins. Photosynth Res 63:85–96

Green BR, Parsons WW (2003) Light-harvesting systems in chlorophyll c-containing algae. In: Light-harvesting antennas in photosynthesis. Advances in photosynthesis and respiration, vol 13, Kluwer Academic Publishers, Dordrecht, Boston, London, pp 324–348

Guglielmi G, Lavaud J, Rousseau B, Etienne A, Houmard, Ruban A (2005) The light-harvesting antenna of the diatom *Phaeodactylum tricornutum* evidence for a diadinoxanthin-binding subcomplex. FEBS J 272:4339–4348

Harauz G, Boekema EJ, van Heel M (1988) Statistical image analysis of electron micrographs of ribosomal subunits. Methods Enzymol 164:35–49

Hiller RG, Anderson JM, Larkum AWD (1991) The chlorophyll-protein complexes of algae. In: Scheer H (ed) Chlorophylls. CRC Press, Boca Raton, FL, pp 530–547

Ikeda Y, Komura M, Watanabe M, Minami C, Koike H, Itoh S, Kashino Y, Satoh K (2008) Photosystem I complexes associated with fucoxanthin-chlorophyll-binding proteins from a marine centric diatom, *Chaetoceros gracilis*. Biochim Biophys Acta 1777:351–361

Jordan P, Fromme P, Witt HT, Klukas O, Saenger W, Krauss N (2001) Three-dimensional structure of cyanobacterial photosystem I at 2.5 Å resolution. Nature 411:909–917

Joshi-Deo J, Schmidt M, Gruber A, Weisheit W, Mittag M, Kroth P, Buchel C (2010) Characterization of a trimeric light-harvesting complex in the diatom *Phaeodactylum tricornutum* built of FcpA and FcpE proteins. J Exp Bot 61:3079–3087

Kargul J, Nield J, Barber J (2003) Three-dimensional reconstruction of a lightharvestingcomplex I—photosystem I (LHCI-PSI) supercomplex from the green alga *Chlamydomonas reinhardtii*. J Biol Chem 278:16135–16141

Katoh T, Ehara T (1990) Supramolecular assembly of fucoxanthin-chlorophyll protein complexes isolated from a brown alga, *Petalonia fascia*. Electron microscopic studies. Plant Cell Physiol 31(4):439–447

Katoh H, Mimuro M, Takaichi S (1989) Light-harvesting particles isolated from a brown alga, *Dictyota dichotoma.* A supramolecular assembly of fucoxanthin-chlorophyll-protein complexes. Biochim Biophys Acta 976:233–240

Koenig F, Schmidt M (1995) *Gloeobacter violaceus*—investigation of an unusual photosynthetic apparatus. Absence of the long wavelength emission of photosystem I in 77 K fluorescence spectra. Physiol Plant 94:621–628

Kruip J, Chitnis PR, Lagoutte B, Rogner M, Boekema EJ (1997) Structural organization of the major subunits in cyanobacterial photosystem I. Localization of subunits PsaC, -D, -E, -F, and–J. J Biol Chem 272:17061–17069

Kuhl H, Rogner M, van Breemen JF, Boekema EJ (1999) Localization of cyanobacterial photosystem II donor-side subunits by electron microscopy and the supramolecular organization of photosystem II in the thylakoid membrane. Eur J Biochem 266:453–459

Lepetit B, Volke D, Szabo M, Hoffmann R, Garab G, Wilhelm Ch, Goss R (2007) Spectroscopic and molecular characterization of the oligomeric antenna of the diatom *Phaeodactylum tricornutum*. Biochemistry 46:9813–9822

Lichtenthaler KH (1987) Chlorophylls and carotenoids: pigments of photosynthetic biomembranes. Methods Enzymol 148:350–385

Loll B, Kern J, Saenger W, Zouni A, Biesiadka J (2005) Towards complete cofactor arrangement in the 3.0 Å resolution structure of photosystem II. Nature 438:1040–1044

Mimuro M, Katoh T, Kawai H (1990) Spatial arrangement of pigments and their interaction in the fucoxanthin/chlorophyll a/c protein assembly (FCPA) isolated from the brown alga *Dictyota dichotoma.* Analysis by means of polarized spectroscopy. Biochim Biophys Acta 1015:450–456

Mimuro M, Ookubo T, Takahashi D, Sakawa T, Akimoto S, Yamazaki I, Miyashita H (2002) Unique fluorescence properties of a cyanobacterium *Gloeobacter violaceus* PCC 7421: reasons for absence of the long-wavelength PSI Chl a Fluorescence at –196°C. Plant Cell Physiol 43:587–594

Ogawa T, Vernon LP (1971) Increased content of cytochromes 554 and 562 in *Anabaena variabilis* cells grown in the presence of diphenylamine. Biochim Biophys Acta 226:88–97

Owens TG, Wold ER (1986) Light-harvesting function in the diatom *Phaeodactylum tricornutum.* I. Isolation and characterization of pigment-protein complexes. Plant Physiol 80:732–738

Passaquet C, Thomas JC, Caron L, Hauswirth N, Puel F, Berkaloff C (1991) Light-harvesting complexes in brown algae. Biochemical characterization and immunological relationships. FEBS Lett 280:21–26

Pyszniak AM, Gibbs SP (1992) Immunocytochemical localization of photosystem I and the fucoxanthin-chlorophyll a/c light-harvesting complex in the diatom *Phaeodactylum tricornutum*. Protoplasma 166:208–217

Rogner M, Muhlenhoff U, Boekema EJ, Witt HT (1990) Monomeric, dimeric and trimeric PSI reaction center complex isolated from the thermophilic cyanobacterium *Synechococcus* sp.-size, shape and activity. Biochim Biophys Acta 1015:415–424

Vacha F, Bumba L, Kaftan D, Vacha M (2005) Microscopy and single molecule detection in photosynthesis. Micron 36:483–502

van den Hoek C, Mann DG, Jahns HM (1995) Algae. An Introduction to phycology. Cambridge University Press, Cambridge

van der Staay GW, Boekema EJ, Dekker JP, Matthijs HCP (1993) Characterization of trimeric Photosystem I particles from the prochlorophyte *Prochlorothrix hollandica* by the electron microscopy and image analysis. Biochim Biophys Acta 1142:189–193

van Heel M, Frank J (1981) Use of multivariate statistics in analyzing the images of biological macromolecules. Ultramicroscopy 6:187–194

Veith T, Buchel C (2007) The monomeric photosystem I-complex of the diatom *Phaeodactylum tricornutum* binds specific fucoxanthin chlorophyll proteins (FCPs) as light-harvesting complexes. Biochim Biophys Acta 1767:1428–1435

Whittle SJ, Casselton JP (1975) The chloroplast pigments of the algal classes Eustigmatophyceae and Xanthophyceae, II. Xanthophyceae. Eur J Phycol 10:192–204

Wilhelm C, Buchel C, Rousseau B (1988) Molecular organization of chlorophyll-protein complexes in the xanthophycean alga *Pleurochloris meiringensis*. Biochim Biophys Acta 934: 220–226